

## Precise Motion Control for Magnetically Levitated Stage

### Katsuhide Watanabe

Ebara Corporation, Fujisawa, Kanagawa-Pref., 251-8502 Japan  
[Watanabe.Katsuhide@ebara.com](mailto:Watanabe.Katsuhide@ebara.com)

### Ichiju Satoh

Ebara Corporation, Fujisawa, Kanagawa-Pref., 251-8502 Japan  
[Satoh.Ichiju@ebara.com](mailto:Satoh.Ichiju@ebara.com)

### Takahide Haga

Ebara Corporation, Fujisawa, Kanagawa-Pref., 251-8502 Japan  
[Haga.Takahide@ebara.com](mailto:Haga.Takahide@ebara.com)

### Shunichi Aiyoshizawa

Ebara Corporation, Fujisawa, Kanagawa-Pref., 251-8502 Japan  
[Aiyoshizawa.Shunichi@ebara.com](mailto:Aiyoshizawa.Shunichi@ebara.com)

### ABSTRACT

An attempt was made to develop a magnetically levitated fine motion stage capable of super-fine, nm-level positioning. This non-contact stage, used for placing samples, includes a magnetic actuator for fine positioning control, as well as displacement sensors for detecting stage positions. The stage also features a magnetic shield housing for minimizing magnetic field effects outside the stage. A DSP controller, featuring robust control based on a 2-degree-of-freedom  $H_\infty$  theory is applied for improved accuracy positioning and servo performance in high frequency regions. The stage is capable of 6-degrees-of-freedom control. Positioning tests, conducted at micrometer to nanometer level positioning, indicated a possibility that the developed stage could be used over a wide range of precision positioning.

### INTRODUCTION

High performance and reliability of semiconductor manufacturing and inspection systems are sought today to meet the demand for higher precision in semiconductor design tools. Precision control in semiconductor manufacturing processes have now shifted from the micrometer level to the nanometer level. As was indicated in the International Technology Roadmap for Semiconductors (ITRS) 2000, precision machining of semiconductors is expected to further progress. Under such background, there is high demand for R & D on precise positioning, including that using magnetic levitation. Accordingly, there is much R & D in progress for precise positioning which makes use of magnetic levitation characteristics.

The research conducted herein involved tests of a prototype magnetically levitated fine motion stage capable of 6-degrees-of-freedom(6-DOF), super-fine nm-level positioning, including its control responses. The magnetic force in this stage is insulated and therefore the influence of magnetic field outside the stage is

minimized. Robust control based on a 2-DOF  $H_\infty$  theory and the model matching method is applied for improved accuracy positioning and servo performance in high frequency ranges. Positioning tests, conducted at micrometer to nanometer level positioning, indicated a possibility that the developed stage could be used over a wide dynamic range of precision positioning and with high-speed responsiveness. The following outlines the test results.

### MECHANICAL DESCRIPTION

Photo 1 shows the magnetically levitated fine motion stage system, while Figure 1 shows its geometry. The stage system includes the levitation stage for placing specimen, an actuator (electromagnets and permanent magnets) for non-contact support of the levitation stage and controlling the fine positioning, and displacement sensors for detecting the levitation stage position. The levitation stage is made up of a plane section for placing specimen and the four sides which slope down from the four corners of the stage. The bottom section constitutes

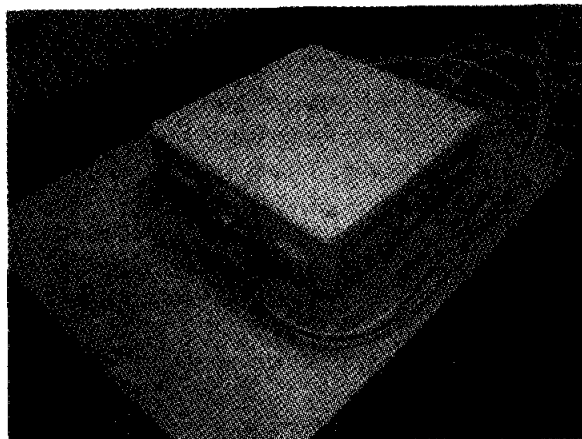


PHOTO 1: View of magnetically levitated stage system

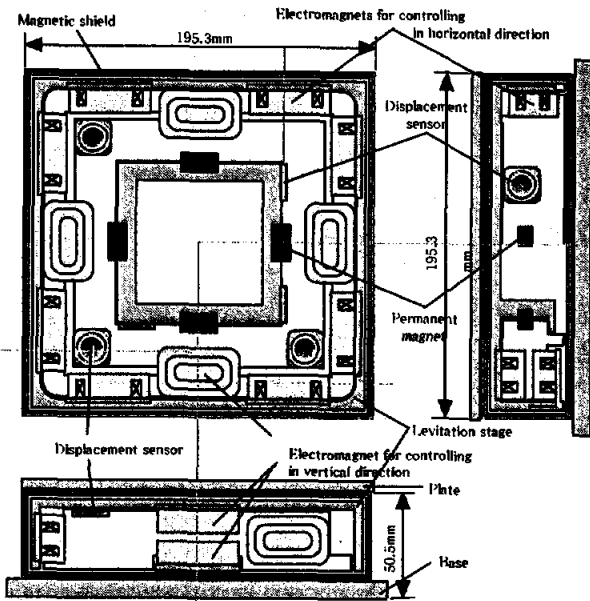


FIGURE 1: Construction of magnetically levitated fine motion stage system

an open box shape. Target magnet poles of electromagnets and permanent magnets are set inside the stage. The base portion is surrounded by the box-shape stage includes the permanent magnets and electromagnets, as well as displacement sensors. The periphery of the stage and housing is covered by a magnetic shield layer to minimize the outing of magnetic field. Electromagnets are set on the periphery of the base, while permanent magnets are set at the central section of the stage, thus allowing the stage to remain low. The permanent magnets work to keep the temperature of electromagnets down during magnetic levitation. This results in supporting the dead weight of the levitation stage and the electromagnets control the fine displacement in the equilibrium point. Six displacement sensors (capacity type: resolution of 3 nm and bandwidth of 2 kHz) are also set in the base section.

## MODERING

### Numerical Model

In this section, we obtain a low-dimension model with 6-DOF, assume that the levitation stage is rigid.

**Geometry of the model.** Figure 2 shows the magnetically levitated fine motion stage model. The stage is supported by 16 electromagnets and 4 sets of laminated permanent magnets. The displacement sensors for the positioning are set in different locations from those of the electromagnets.

**Nomenclature.** The symbols used in figures and equations are as shown below.

$m$	Levitated mass
$I_x, I_y, I_z$	Moment of inertia for center of mass

$F_x, F_y, F_z, F_{\alpha}, F_{\beta}, F_{\gamma}$	Control forces and moments of control forces
$W_x, W_y, W_z, W_{\alpha}, W_{\beta}, W_{\gamma}$	External forces
$x, y, z$	Displacement of levitation stage's center of gravity position
$\alpha, \beta, \gamma$	Angle displacement of levitation stage's center of gravity
$u, v, w$	Displacement at base
$\xi, \eta, \zeta$	Angle displacement at base
$a_{xi}, a_{yi}, a_{zi} (i = 1 \sim 4)$	Coordinates of the elastic support position
$b_{xi}, b_{yi}, b_{zi} (i = 1 \sim 8)$	Coordinates of the electromagnet's point of application
$d_{xi}, d_{yi}, d_{zi} (i = 1 \sim 6)$	Coordinates of the displacement sensor's point of detection

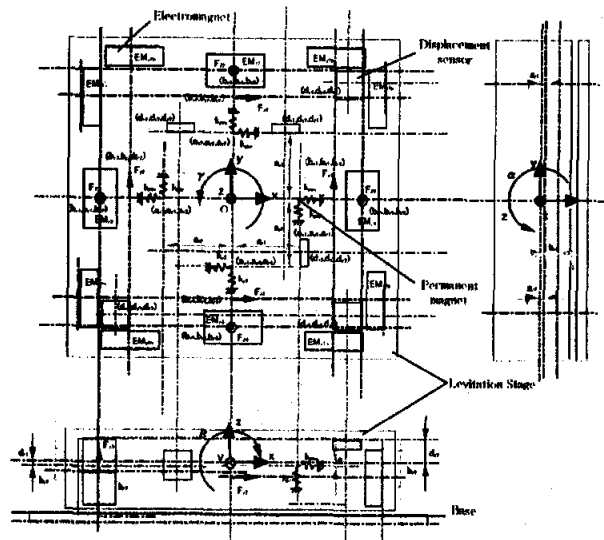


FIGURE 2: Model of magnetically levitated fine motion stage system

**Equations of motions.** The equation of motion in the center of gravity rotation is expressed in Equation (1) below. It shows the equilibrium of the rigid table which is elastically supported by the permanent magnets and electromagnets. The equation indicates that the translation motion in the z-axis direction and its rotational motion around the axis are independent. However, there is a coupling between the translation motion in the y direction and the rotational motion around the x-axis, as well as the translation motion in the x direction, and the rotational motion around the y-axis.

$$M\ddot{X} + C_p\dot{X} + K_p X = F + W \quad (1)$$

$$W = -MX_g$$

$$X = X_p - X_g$$

$$X_p = [x \ y \ z \ \alpha \ \beta \ \gamma]^T$$

$$X_g = [u \quad v \quad w \quad \xi \quad \eta \quad \zeta]^T$$

$$F = [F_x \quad F_y \quad F_z \quad F_\alpha \quad F_\beta \quad F_\gamma]^T$$

$$W = [W_x \quad W_y \quad W_z \quad W_\alpha \quad W_\beta \quad W_\gamma]^T$$

In the above  $M$  is the mass matrix,  $C_p$  is the damping matrix,  $K_p$  is the robustness matrix,  $F$  is the control force vector,  $W$  is the disturbance vector,  $X$  is the relative displacement vector,  $X_p$  is the center of gravity displacement vector, and  $X_g$  is the base displacement vector.

Linearizing at the proximity of a balance condition (control current and displacement), the control force vector in the center of gravity can be expressed as in the following equation.

$$F = B_f(K_u B_s X + K_c I_c) = K_{uc} X + K_{cc} I_c \quad (2)$$

In the above,  $K_u$  is the imbalance stiffness matrix of each electromagnet,  $K_c$  is the control stiffness matrix,  $I_c$  is the control current vector,  $B_s$  is the displacement conversion matrix from the center of gravity position to the actuator applying position,  $B_f$  is the force transform matrix from the application point of the electromagnet to the center of gravity position. From this the equation (1) can be expressed as the following.

$$M\ddot{X} + C_p\dot{X} + (K_p - K_{uc})X = K_{cc}I_c - MX_g \quad (3)$$

### Controlled Object Model

A controlled object model was made for the design of the control system. A transformation is made here from the physical coordinate system to a mode coordinate system for realizing a completely decoupling, 6-DOF rigid body. We can design control system of each DOF by using this model. The motion equation which is transformed to mode coordinate system is expressed as the following.

$$\ddot{\eta} + 2[\zeta][\Omega]\dot{\eta} + [\Omega]^2\eta = \Phi^T F_c - \Phi^T M\ddot{X}_g \quad (4)$$

$$x_m = \eta + w_m \quad (5)$$

Regarding  $\eta$  is the mode displacement,  $\Phi$  is the mode matrix normalized in terms of mass.  $[\zeta]$  is the mode damping ratio,  $[\Omega]$  is the mode eigenvalue. And  $x_m$  is absolute mode displacement. If we have Laplace transform Equations (4) and (5) without disturbance, we can obtain transfer functions for controlled object in each 6-DOF independently.

$$x_{mr}(s) = \frac{1}{s^2 + 2\zeta_r\Omega_r s + \Omega_r^2} f_{mr} \quad (r=1\sim6) \quad (6)$$

$$f_{mr} = \Phi^T F_c = \Phi^T K_{cc} I_c$$

$f_{mr}$  is the mode manipulated variable while  $\zeta_r$  is obtained from experimental values.

## DESIGNING THE CONTROL SYSTEM

Figure 3 shows a block diagram of the control system for the magnetically levitated fine motion stage. The controller was designed to control each mode independently. The  $H_\infty$  theory, a representative robust control theory, was used for the design of the control system. A DSP controller, featuring robust control based on a 2-DOF  $H_\infty$  theory is applied for improved accuracy positioning and servo performance in high frequency regions.

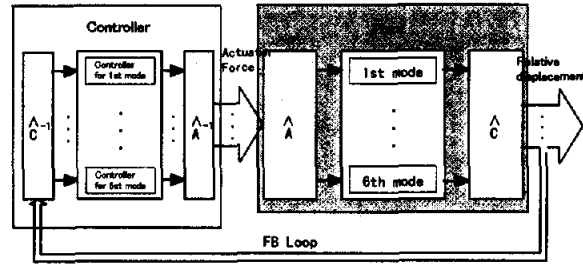


FIGURE 3: Block diagram of control system

### $H_\infty$ Control System

Our objective in the R&D of the magnetically levitated fine motion stage system was to establish a high-precision fine positioning. For instance, when changing the position of the specimen placed on the stage a few millimeters or a few centimeters, a long stroke stage such as an X-Y type needs to be used, in which case the disturbance from the X-Y stage needs to be considered. The controlled object model was assumed rigid however there was an elastic mode on the high frequency region as well as observation noise of displacement sensors, thus making it necessary to consider the effects such had on the stability of the control system. Therefore, an attempt was made to solve such problems by using the  $H_\infty$  theory and determining them as mixed sensitivity problems. The result was a control system with a disturbance suppression feature as well as robust stability. Figure 4 shows the block diagram of an augmented system with a weighting function. The  $P_r(s)$  is the nominal plant per each DOF,  $K_r(s)$  is the controller,  $w_{mr}$  is the disturbance, and  $W_1(s)$  and  $W_2(s)$  are weighting functions.  $P_r(s)$  is the transfer function in Equation (7) for the controlled object model mentioned earlier.

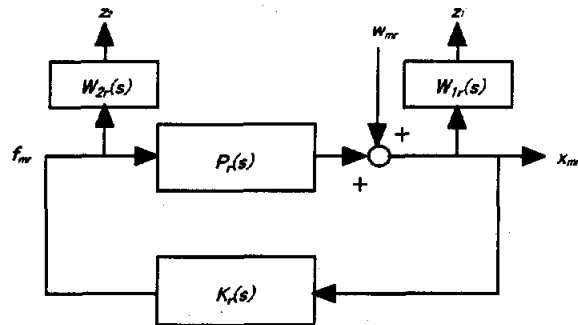


FIGURE 4: Augmented system

$$P_r(s) = \frac{1}{s^2 + 2\zeta_r \Omega_r s + \Omega_r^2} \quad (r = 1 \sim 6) \quad (7)$$

Let us attempt a reduction in sensitivity by assuming the weighting function to be  $W_{1r}(s)$  versus the sensitivity function  $S_r(s)$  between disturbance displacement  $w_{mr}$  and absolute displacement  $z_1$ . Furthermore, let us assume that the model errors in the high frequency region are plant augmentative model errors, and attempt a robust stabilization by assuming the weight function to be  $W_{2r}(s)$  versus the quasi-complementary sensitivity function  $T_{ar}(s)$  between disturbance displacement  $w_{mr}$  and mode manipulated variable  $z_2$ . The weighting functions for each case can be expressed in the following equations.

$$W_{1r}(s) = g_{1r} \frac{T_{s1r}s + 1}{T_{s2r}s + 1} \quad (r=1 \sim 6) \quad (8)$$

$$W_{2r}(s) = g_{2r} \frac{T_{t1r}s + 1}{T_{t2r}s + 1} \quad (r=1 \sim 6) \quad (9)$$

The criterion function obtained from the above can be expressed as the following.

$$\left\| \begin{array}{l} S_r(s)W_{1r}(s) \\ T_{ar}(s)W_{2r}(s) \end{array} \right\|_{\infty} < 1 \quad (r=1 \sim 6) \quad (10)$$

Controller  $K_r(s)$  which satisfies the above criterion function can then be obtained. However,  $S_r$  and  $T_{ar}$  are expressed as the following.

$$S_r = \frac{1}{1 + P_r K_r} \quad (11)$$

$$T_{ar} = \frac{K_r}{1 + P_r K_r} \quad (12)$$

The  $H_{\infty}$  controller  $K_r(s)$  thus obtained was used as a feedback control system, and a 6-DOF control system featuring favorable disturbance suppression and robust stability was developed. However as 3-DOF, in the  $Z$ ,  $\alpha$  and  $\beta$  directions, are stabilized by the magnetic restoring force of permanent magnets, the controlled object became the vibratory system with poles. Accordingly, there was a problem of deterioration in the suppression performance in the closed loop system disturbance due to polar-zero cancellation, when facing the mixed sensitivity problem. As shown in Figure 5, the problem concerning the 3-DOF was designed by the application of an augmented system which featured the introduction of disturbance into the input end of controlled object  $P_r(s)$ .  $w_2$  here was an assumed disturbance applied for satisfying an assumed standard  $H_{\infty}$  control problem. Assuming that  $T_{zw}(s)$  is the closed loop transfer function between the controlled variables ( $z_1$  and  $z_2$ )

and the disturbances ( $w_1$  and  $w_2$ ), the criterion function becomes as indicated in Equation (13). We then sought out the controller  $K_r(s)$  that would satisfy this criterion function.

$$\|T_{zw}(s)\|_{\infty} < 1 \quad (13)$$

Where

$$T_{zw}(s) = \begin{bmatrix} W_{1r}(s)S_{dr}(s) & w_n W_{1r}(s)S_r(s) \\ W_{2r}(s)T_{ar}(s) & w_n W_{2r}(s)T_{ar}(s) \end{bmatrix}$$

$$S_{dr} = \frac{P_r}{1 + P_r K_r}$$

$$T_{ar} = \frac{P_r K_r}{1 + P_r K_r} \quad (r=3 \sim 5)$$

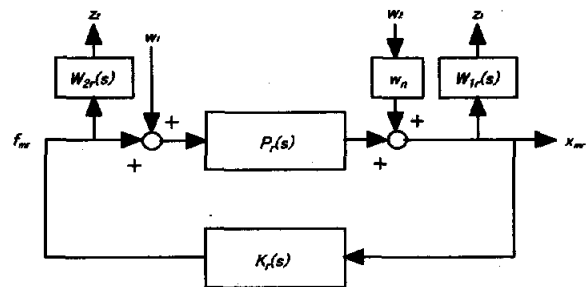


FIGURE 5: Augmented system using disturbance from input end

## 2-DOF $H_{\infty}$ Control System

A 2-DOF  $H_{\infty}$  control system was designed using the model matching method. This control system was designed to be capable of maintaining the disturbance suppression performance and robust stability in the translation  $x$ ,  $y$  and  $z$  directions, thus improving the target response performance. Figure 6 shows the block diagram of this control system. As the magnetically levitated system was stabilized by the  $H_{\infty}$  controller mentioned earlier, a feed forward function was newly added to the stable feedback system based on the model matching method. In case there was either disturbance input into the 2-DOF system or when there were no changes occurring in the controlled system, the feedback controller  $K_r(s)$  did not work. The transfer function, from the command input  $r_{mr}$  to output  $y_{mr}$ , became the

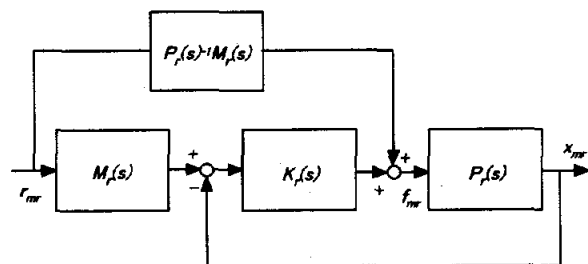


FIGURE 6: 2-DOF control system

set response of model  $M_i(s)$ . The  $M_i(s)$  satisfied the following conditions.

- 1)  $M_i(0) = 1$  for eliminating normal operation errors versus the gradual target values.
- 2) The relative degree of  $M_i(s)$  was set to be higher than that of the controlled system  $P_i(s)$ .

$$M_i(s) = \frac{1}{(T_i s + 1)^n}, \quad i = x, y, z$$

- 3) The frequency characteristics of  $M_i(s)$  were selected with consideration given to the transfer characteristics  $(1 + \tilde{P}_i(s)K_i(s))^{-1}$  from  $r_{mr}$  to  $y_{mr}$ .

The  $\tilde{P}_i(s)$  here indicates the actual controlled object.

## EVALUATION TEST

### Experimental Apparatus

The levitation and positioning test was carried out for the prototype magnetically levitated fine motion stage system. Photo 2 shows the test apparatus. As the positioning test involved nano-levels, the stage system was placed on a vibration isolation system to avoid any disturbance from the floor. Figure 7 shows a block diagram of the control system. A high-speed digital controller (DSP-TMS320C67) was used. A low noise, series dropper was used as the drive circuit for exciting the electromagnets.

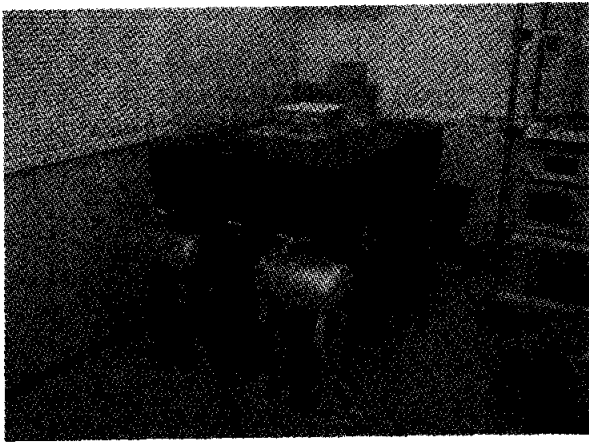


PHOTO 2: Test apparatus

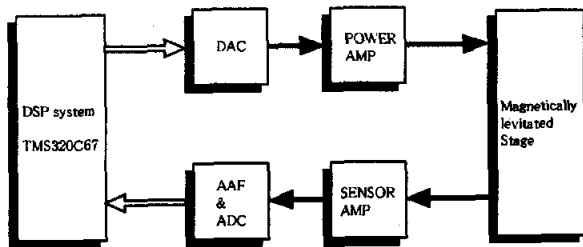
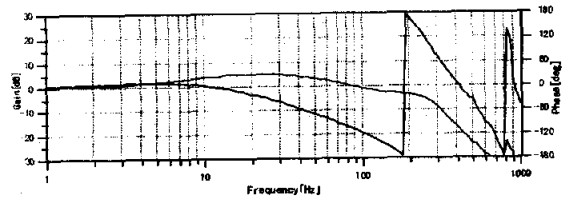


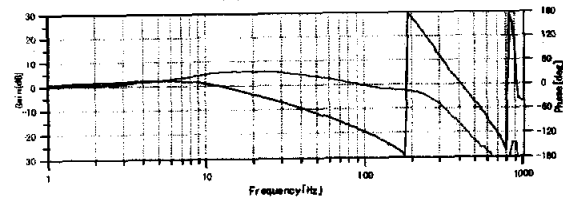
FIGURE 7: Control system

### Frequency Characteristics

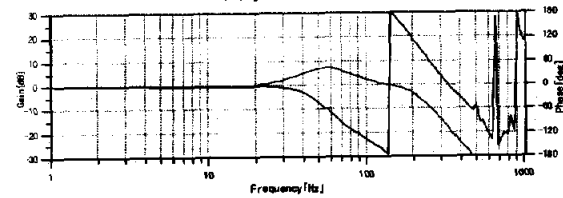
The target responsiveness for the servo system of the magnetically levitated fine motion stage system was 100 Hz. Tests were conducted for normal operation directions (x, y, and z) for a 1-DOF and 2-DOF  $H_\infty$  control systems. Figure 8 shows the frequency characteristics of the 1-DOF control system. The frequency characteristics of the servo system, from the target command value  $r_{mr}$  to mode displacement  $x_{mr}$  for each DOF, are shown. Although stable feedback was indicated for each control system, there was non-conformity with the gain 0dB line (indicating the target follow-up performance) as well as late lags. Figure 9 shows the frequency characteristics of the 2-DOF control system, designed based on the model matching method. The conformity with the gain 0dB line and phase lag had become improved, and the responsiveness of the servo system had become improved as well up to the 200 Hz range.



(a) x direction

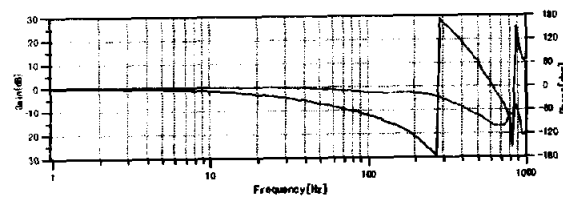


(b) y direction

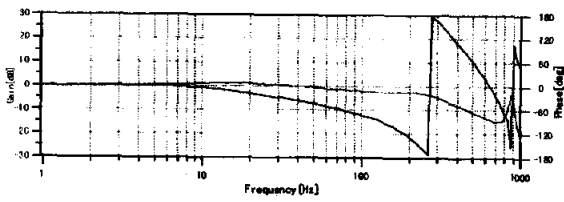


(c) z direction

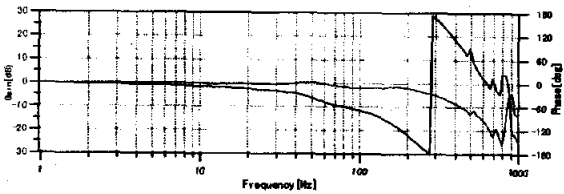
FIGURE 8: Frequency characteristic of 1-DOF control system



(a) x direction



(b) y direction



(c) z direction

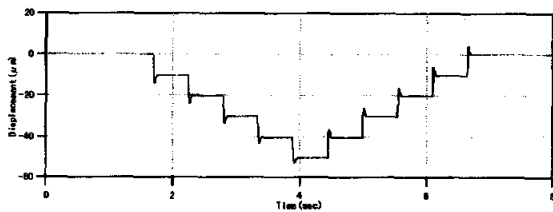
FIGURE 9: Frequency characteristic of 2-DOF control system

### Fine Motion Positioning

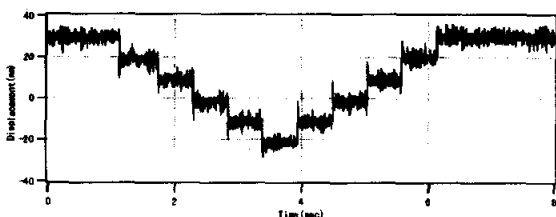
A feature of the magnetically levitated fine motion stage system is that it allows positioning within gaps. Therefore, positioning control becomes possible for relatively large to fine displacement step width, fine motion tests were carried out from  $10 \mu\text{m}$  to  $5 \text{nm}$  displacements. Figures 10 – 12 show positioning test results for translational directions ( x and z directions) and x axis  $\alpha$  direction rotation angle. The envelopes indicated in all figures had been measured within the frequency range of 100 Hz. It can be grasped that the positioning from the micrometer to nanometer levels had been attained, for normal as well as rotational directions.

### CONCLUSION

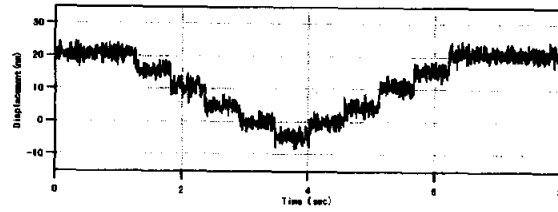
Positioning tests using the newly developed magnetically levitated fine motion stage system indicated that this stage was fully capable for wide-range precision positioning from micrometer to nanometer levels. Non-compound stable control was possible by a DSP controller, featuring robust control based on the  $H_\infty$  theory.



(a)  $10 \mu\text{m}$

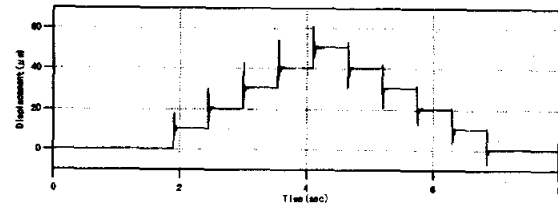


(b)  $10 \text{nm}$

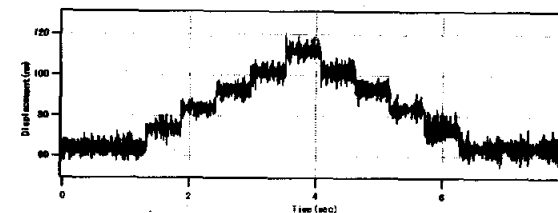


(c)  $5 \text{nm}$

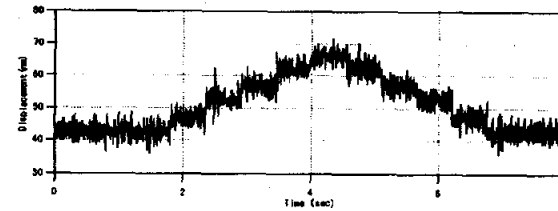
FIGURE 10: Step width positioning in x direction



(a)  $10 \mu\text{m}$



(b)  $10 \text{nm}$



(c)  $5 \text{nm}$

FIGURE 11: Step width positioning in z direction

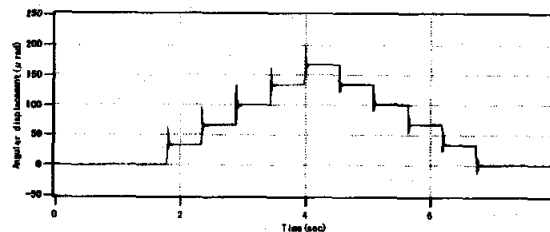


FIGURE 12: Step width positioning in  $\alpha$  direction

A 2-points-of-freedom  $H_\infty$  control system, designed for improving target responsiveness, greatly improved the frequency characteristics of the servo system.

### References

1. International Technology Roadmap for Semiconductors 2000 Update, <http://public.itrs.net/Files/2000UpdateFinal/ORTC2000final.pdf>
2. R.Warling . S.M.Kohler , Six degree of freedom fine motion positioning stage based on magnetic levitation , Second annual symposium on magnetic suspension technology, Seattle, WA., August 11-13 , 1993